

# We are IntechOpen, the world's leading publisher of Open Access books Built by scientists, for scientists

6,900

Open access books available

186,000

International authors and editors

200M

Downloads

Our authors are among the

154

Countries delivered to

TOP 1%

most cited scientists

12.2%

Contributors from top 500 universities



WEB OF SCIENCE™

Selection of our books indexed in the Book Citation Index  
in Web of Science™ Core Collection (BKCI)

Interested in publishing with us?  
Contact [book.department@intechopen.com](mailto:book.department@intechopen.com)

Numbers displayed above are based on latest data collected.  
For more information visit [www.intechopen.com](http://www.intechopen.com)



# Plastic Inorganic Semiconductors for Flexible Electronics

*Tian-Ran Wei, Heyang Chen, Xun Shi and Lidong Chen*

## Abstract

Featured with bendability and deformability, smartness and lightness, flexible materials and devices have wide applications in electronics, optoelectronics, and energy utilization. The key for flexible electronics is the integration of flexibility and decent electrical performance of semiconductors. It has long been realized that high-performance inorganic semiconductors are brittle, and the thinning-down-induced flexibility does not change the intrinsic brittleness. This inconvenient fact severely restricts the fabrication and service of inorganic semiconductors in flexible and deformable electronics. By contrast, flexible and soft polymers can be readily deformed but behave poorly in terms of electrical properties. Recently,  $\text{Ag}_2\text{S}$  was discovered as the room-temperature ductile inorganic semiconductor. The intrinsic flexibility and plasticity of  $\text{Ag}_2\text{S}$  are attributed to multicentered chemical bonding and solid linkage among easy slip planes. Furthermore, the electrical and thermoelectric properties of  $\text{Ag}_2\text{S}$  can be readily optimized by Se/Te alloying while the ductility is maintained, giving birth to a high-efficiency full inorganic flexible thermoelectric device. This chapter briefly reviews this big discovery, relevant backgrounds, and research advances and tries to demonstrate a clear structure-performance correlation between crystal structure/chemical bonding and mechanical/electrical properties.

**Keywords:** flexible electronics, plastic inorganic semiconductors, chemical bonds

## 1. Introduction

Flexible electronics endows electronic circuits with novel flexibility, foldability, and scalability, breaking the restriction of wafers and greatly expanding the application in various fields, e.g., flexible displays, electronic textiles, and sensory skins [1–3]. Consequently, flexible electronics has attracted widespread attention from both academic and industrial communities and has witnessed marvelous breakthroughs in terms of material development [4–5], device fabrication, packaging, and integration [6–8].

In flexible electronics, semiconductors and devices are mounted onto flexible substrates, mostly polymers [1, 9]. The key to flexible electronics is realizing both high flexibility and desired physical/chemical properties (mostly electrical performance) of the semiconductors. Due to the intrinsic softness and flexibility, polymer semiconductors have long been a popular candidate for flexible electronics [10–13]. However, carriers in organic materials are rather localized, leading to poor electrical conduction. Another way to realize “flexibility” is to process inorganic materials into ultrathin format to reduce the stiffness [5, 14], and this is why 2D materials or thin films are widely used [15–16]. However, the thinning-induced flexibility does

not change the intrinsic brittleness and rigidity [17–18] of the inorganic semiconductors, which are constituted mainly by covalent or ion-covalent bonding [19].

Regarding this issue, another important mechanical property, plasticity, should be considered. As a matter of fact, however, plasticity is a long-sought target for inorganic materials, e.g., ceramics [20]. On the one hand, plasticity means machinability, that is, plastic ceramics can be mechanically deformed and processed just like metals do. On the other hand, plastic deformation can prevent the sudden, catastrophic, brittle fracture, which is essential to not only structural materials but also functional materials. Hence, the discovery of the room-temperature plastic inorganic semiconductor  $\text{Ag}_2\text{S}$  [21] and the fabrication of full-inorganic  $\text{Ag}_2\text{S}$ -based thermoelectric (TE) power generation modules [22] are ground breaking, opening a new avenue toward next-generation flexible electronics.

This chapter will provide an in-time overview for the newly discovered plastic/flexible inorganic semiconductors. We shall first clarify the concept of flexibility and then illustrate the intrinsic plasticity for metals and brittleness for inorganic materials. Then, we will mention the special plasticity and the chemical bonding origins in a few ionic crystals such as  $\text{AgCl}$ . After that, we will systematically review the extraordinary mechanical properties of  $\text{Ag}_2\text{S}$  and fully flexible thermoelectric devices. Finally, the prospect and challenge for plastic inorganic semiconductors as flexible electronic materials will be discussed.

## 2. Fundamental concepts: flexibility

As a matter of fact, “flexibility,” unlike “ductility” or “rigidity,” is not a scientifically clear concept. For flexible electronics, it is widely conceived that only elastic deformation is needed or allowed. In this sense, “flexibility” refers to the ability of the material/device to bend easily in an elastic way. According to Peng and Snyder [23], flexibility  $f$  is quantified by the largest curvature of bending,  $1/r_b$ , where  $r_b$  is the minimum bending radius. A material with a thickness  $h$  bent about a radius  $r_b$  experiences the greatest tensile and compressive stresses on the outer and inner faces, respectively. The maximum strain is readily calculated from the geometry considering that the middle (neutral layer) of the material is unstrained:

$$\varepsilon = \frac{\left[2\pi\left(r_b + \frac{h}{2}\right) - 2\pi r_b\right]}{2\pi r_b} = \frac{h}{2r_b} \quad (1)$$

The maximum elastic strain is reached when plastic deformation occurs:  $\varepsilon = \sigma_y/E$ , where  $E$  is the elastic (Young’s) modulus. Thus, the flexibility becomes:

$$f = \frac{1}{r_b} = \frac{2}{h} \varepsilon_y = \frac{2}{h} \frac{\sigma_y}{E} \quad (2)$$

Removing the shape factor ( $2/h$ ), the material flexibility is  $f_{\text{form}} = \sigma_y/E$ .

The value of  $f_{\text{form}}$  is plotted in **Figure 1** for various materials. It is seen that this definition with the plot well distinguishes commonly sensed flexible materials such as rubber between rigid ones like ceramics. In fact, this definition is essentially consistent with the commonly seen bending stiffness or flexural rigidity,  $f_r \sim h^3 E$  [14, 24]. That is, intrinsically stiff materials with a large thickness tend to be rigid or not flexible. Accordingly, (elastic) flexibility can be realized in thin films or flakes. Therefore, two-dimensional (2D) materials are popular candidates for flexible electronics.

The above definition treats flexibility as elastic deformability, which is reasonable considering the real application. However, as discussed in Section 1, plasticity is important, particularly for efficient material processing. A plastic material can be easily processed into target geometry with little fracture or waste. In addition,

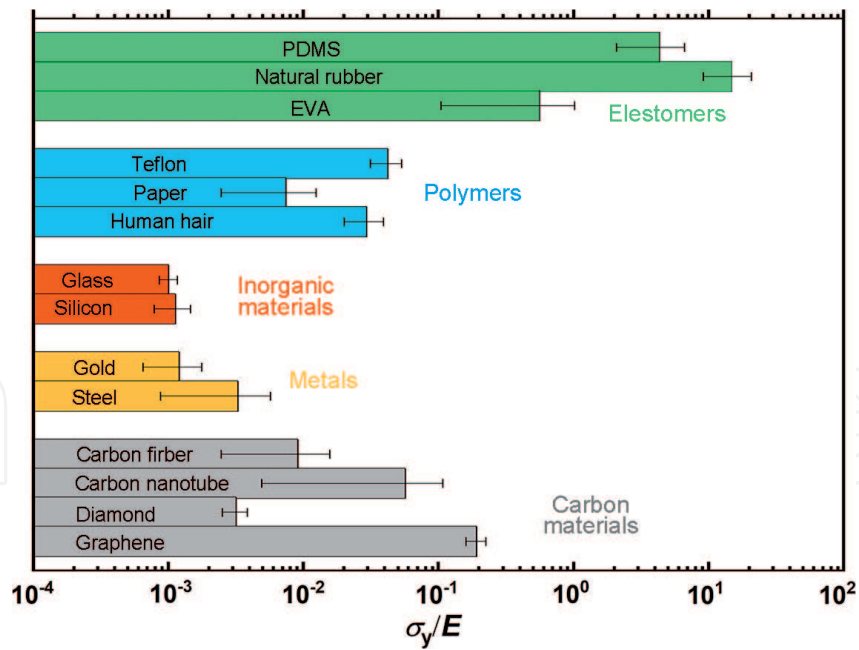


**Figure 1.**  
 The ratio of yield strength to Young's modulus for various materials. Raw data are taken from Ref. [23].

a plastic material gains intrinsic flexibility without the restrict of size, that is, it can be readily deformed without breaking even in the bulk format, which is essentially important for applications requiring energy densities. Nonetheless, plasticity is rarely seen in inorganic semiconductors, which will be discussed in Section 3.

### 3. Prevalent brittleness for inorganic semiconductors

Ductile and brittle behaviors are schematically shown in **Figure 2(a)**. Inorganic semiconductors are mostly constituted by covalent or ion-covalent bonds [25], which assure an appreciable electron orbital overlap, dispersive electronic band, and decent carrier mobility [26]. Covalent bonds are directional, saturated, and localized. Therefore, even a trivial bonding distortion will cause a large instability, which is vividly demonstrated by the deep and steep curve in the interatomic potential versus

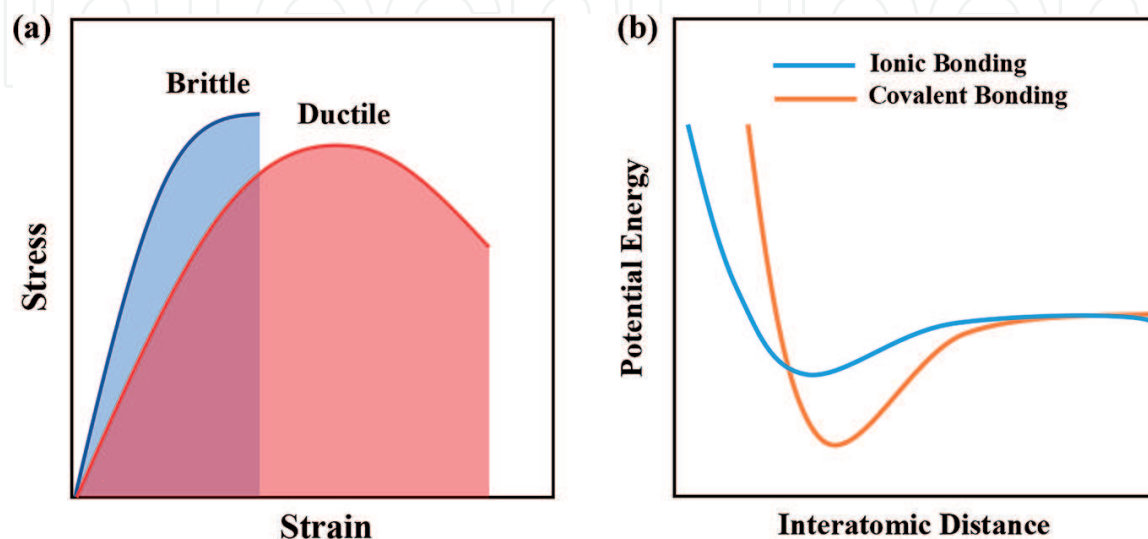


**Figure 2.**  
 (a) Stress-strain curves for brittle and ductile materials and (b) atomic potential varying with atomic distances.

atomic distance diagram (**Figure 2(b)**) [20]. As a contrast, ionic bonding is unidirectional and nonsaturated. The columbic force is somewhat diffuse and extended within a large space. Consequently, the bonding distortion will induce a smaller variation in energy, as reflected by the shallow and flat potential-distance curve [20]. Nonetheless, charges in ionic materials are localized around anions, leading to a poor electrical conductivity. Metallic bonding strength is mediate between covalent and ionic bonds. Metal atoms use their outer-shell electrons for two- and multicenter polar interactions, which open the possibility to unite charge transfer with a nonnegligible density of states at the Fermi level. This makes up good electrical conductivity and ductility.

Beyond the covalent bonding characteristics, the absence of plasticity and flexibility in inorganic materials can be interpreted in terms of dislocations. Various defects exist in inorganic materials (e.g., ceramics) such as vacancies, interstitials, and voids, strongly inhibiting the movement of dislocations. In addition, grain boundaries can cause dislocation pile-up, which may be a kind of crack source. For metals, the pile-up of dislocations near grain boundaries will cause hardening in mechanical properties. For ceramics, ductility is limited by crack nucleation and glide. In fact, the main deformation mechanism for most ceramics is creep. This process is mainly controlled by dislocation climb and diffusion, both of which are strongly dependent on temperature.

#### 4. Plastic ionic inorganic materials

Although most inorganic materials are generally brittle, some ionic crystals have been found to exhibit some degree of plasticity upon certain deformation even at room temperature, such as AgCl [27–28], KCl [29], and LiF [30]. Under a slow strain rate, these crystals exhibit tensile properties like metals and show the phenomenon of neck down [29]. This ductile behavior is attributed to the wavy slip [31–32]. During the deformation, each grain has its own change and should conform to the distortion of neighbors [33]. The wavy slipping allows to change planes in the vicinity of grain boundaries to permit distortions. The ability of crystals to relax the stress is essential for such a ductile deformation. At higher temperature, dislocations near the grain boundaries are easier to change the slipping planes due to the thermal active diffusion mentioned above, spreading out from boundaries to another grain. Thus, plastic deformation above transition temperature is mainly caused by the increase in slip systems and the dislocate-diffusion-induced creep and cross-slip.

First-principle calculations have been performed to compare the plasticity between AgCl and NaCl [34]. The generalized stacking fault energy (GSFE) and the double of the surface energy  $2\gamma_s$  were used as slipping barrier energy and cleavage energy, respectively. If  $GSFE > 2\gamma_s$ , rupture occurs. It was found that in NaCl,  $GSFE > 2\gamma_s$  happens before reaching the middle of slipping process for most slipping systems. While for AgCl, interestingly, GSFE remains smaller than  $2\gamma_s$  over the whole slipping process for  $\langle 110 \rangle$ ,  $\{110\}$ ,  $\{111\}$ ,  $\{001\}$  systems. It means that the three slipping systems are stable for plastic deformation in AgCl.

The reason for the different plastic behaviors between NaCl and AgCl was further attributed to their fundamental differences in electronic structures (**Figure 3**). The calculations [34] show that the smaller band gap and larger atomic-orbital overlap (Ag-5s and Cl-3p) contribute to a weak ionic bonding in AgCl. Crystal Orbital Hamilton population (COHP) analysis shows that the energies of initial Ag-Cl bonds gradually decrease as slipping proceeds. Particularly, in the (110), (111) planes, new Ag-Cl bonds are formed; a strong Ag-Ag bond is also formed when slipping on (100) planes. These newly formed bonds lower the unstable GSF energies in these slipping systems. While in NaCl, no newly formed bonds are observed.

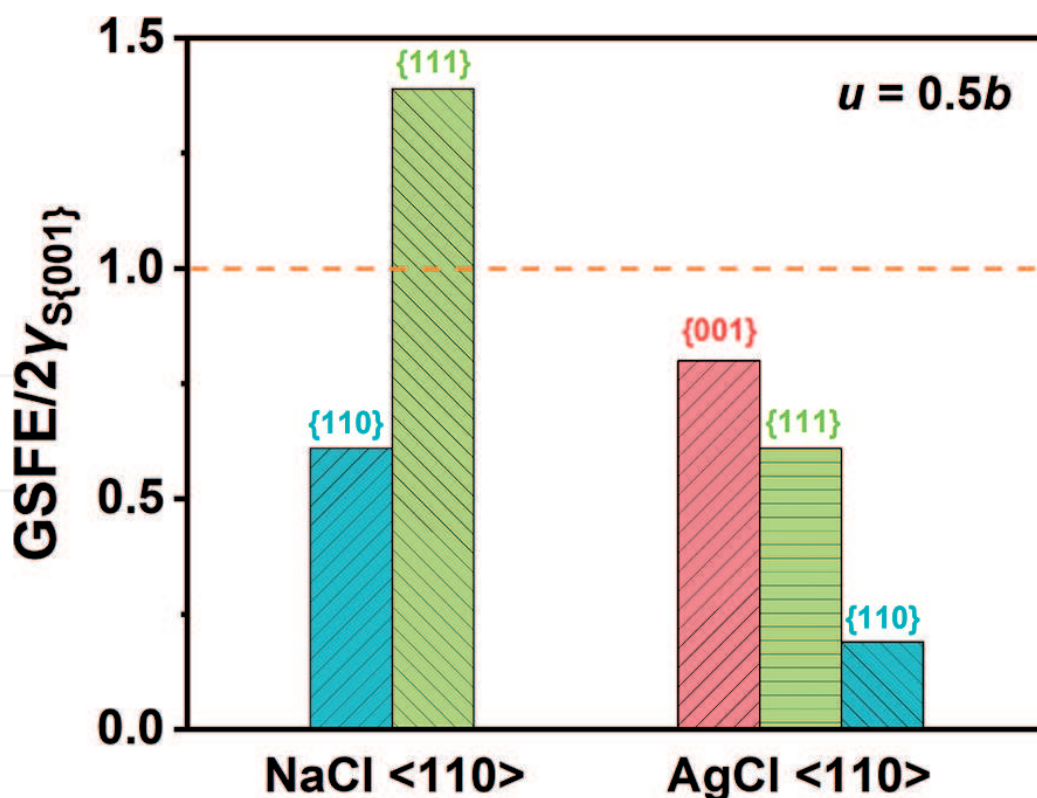


**Figure 3.** The ratio of GSF energy to the double surface energy  $2\gamma_{S\{001\}}$  of the  $\{001\}$  plane for different slipping systems in NaCl and AgCl.  $u$  denotes displacement, and  $b$  is the Burgers vector. The data are taken from Ref. [34].

The plasticity in AgCl was also understood from the perspective of dislocations [35]. Electronic structures of dislocations in AgCl exhibit larger bonding interactions between atomic orbitals than that of NaCl. Also, the nearest neighbor distances around the dislocation core are tend to be shorter than that in NaCl. The two properties lead to a lower core energy ( $E_{\text{core}}$ ) for AgCl. Far from the core, atoms are displaced elastically, and the energy stored elastically ( $E_{\text{elastic}}$ ) for AgCl is also estimated to be lower than that in NaCl. The dislocation excess energies ( $E_{\text{elastic}} + E_{\text{core}}$ ) in NaCl are at least two times higher than that in AgCl, regardless of the type of dislocation. Therefore, it is expected that dislocations in AgCl are much easier to nucleate and multiply from various sources.

## 5. Plasticity of ZnS in darkness

Very recently, ZnS, a well-known brittle material, was also reported to exhibit extraordinary “plasticity” in complete darkness [36]. ZnS crystals fractured immediately when they deformed under light irradiation. However, the crystals could be plastically deformed to a compression strain of 45% in complete darkness as shown in **Figure 4**. It is also found that the optical band gap decreased by 0.6 eV after deformation as also clearly reflected by the apparent colors, which is probably due to the formation of extra energy levels at the bandgap edge in the presence of dislocations.

Based on optical and electronic microscopies, the plastic deformation in complete darkness is caused by glide and multiplication of dislocations belonging to the primary slip system. By contrast, plastic deformation under light irradiation involves deformation twinning. Obviously, the latter corresponds to a much poorer plasticity.

The origins for different deformation types are explained below. The dislocations in ZnS decompose into two partial dislocations. In darkness, the synergetic

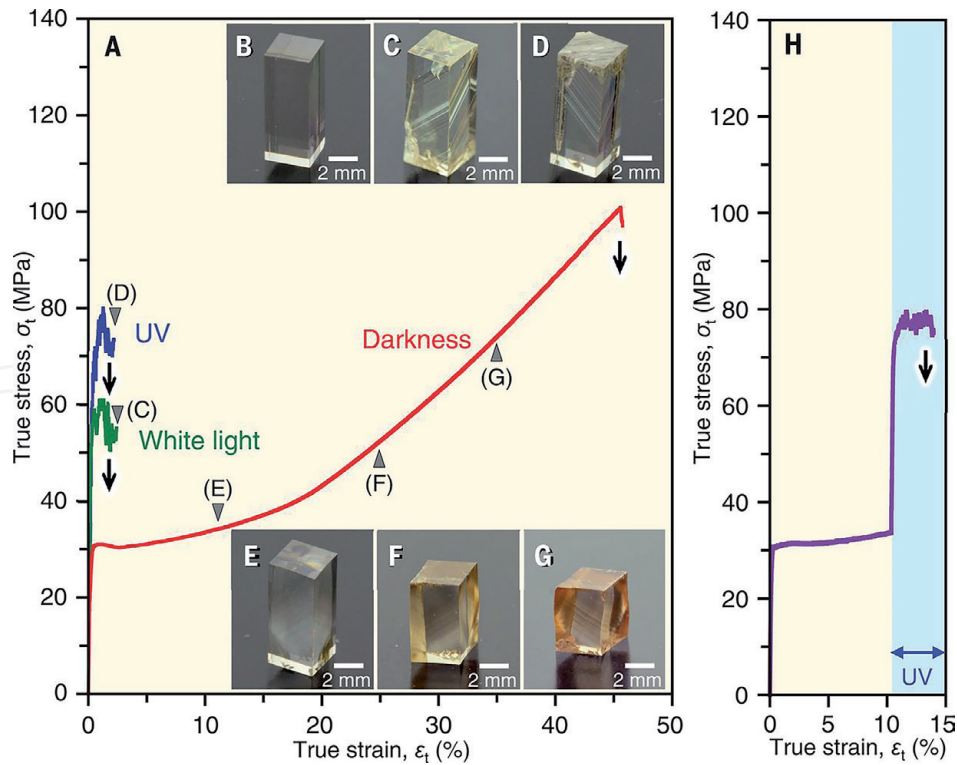


**Figure 4.**

Characterizations of plastic deformation. (a) Stress-strain curves of ZnS single crystals under white or UV light (365 nm) or in complete darkness. (b) An undeformed specimen. (c and d) The specimens deformed under (c) white light-emitting diode (LED) light and (d) UV LED light (365 nm). (e–g) The specimens deformed up to (e)  $\epsilon = 11\%$ , (f)  $\epsilon = 25\%$ , and (g)  $\epsilon = 35\%$  in complete darkness. (h) A stress-strain curve obtained by a deformation in complete darkness up to  $\epsilon = 10\%$  and the subsequent deformation under UV light. Adapted from Ref. [36] with the permission from AAAS, Copyright 2019.

glide motion of the two partials will cause large slip deformations. On the contrary, under light irradiation, photo-excited electrons or holes can be trapped, thus charging some dislocations. The mobility of the dislocation can be limited by dragging the surrounding charge cloud compensating the dislocation charge. Therefore, the different charge states of the two dislocations in ZnS will lead to the great difference of their mobility, which will lead to the observed deformation twinning.

The work suggests that the mechanical properties are strongly intercorrelated to optical and electronic properties. It also implies that inorganic semiconductors are not necessarily “intrinsically” brittle.

## 6. Room-temperature plastic semiconductor Ag<sub>2</sub>S

The plastic ionic materials like AgCl are nearly insulating and cannot be used as semiconductors. Recently,  $\alpha$ -Ag<sub>2</sub>S was discovered as the room-temperature ductile inorganic semiconductor as shown in **Figure 5** [21]. The plasticity of Ag<sub>2</sub>S is extraordinary: the engineering strains are  $\sim 4.5\%$  in tension, 50% in compression, and above 20% in three-point bending, typical characteristics of metals as shown in **Figure 6**.  $\alpha$ -Ag<sub>2</sub>S is a typical nondegenerate *n*-type semiconductor with a low electron carrier concentration about  $(10^{14}\text{--}10^{15})\text{ cm}^{-3}$  and a large, negative Seebeck coefficient (around  $-1000\text{ }\mu\text{V/K}$ ) at room temperature. The band gap is around 1 eV, and RT electrical conductivity ranges from  $0.09$  to  $0.16\text{ Sm}^{-1}$ . The carrier mobility  $\mu_H$  is around  $100\text{ cm}^2/\text{Vs}$  [21].

The marvelous plasticity of  $\alpha$ -Ag<sub>2</sub>S comes from its special crystal structure.  $\alpha$ -Ag<sub>2</sub>S adopts a monoclinic symmetry with the space group  $P2_1/c$ , consisting of

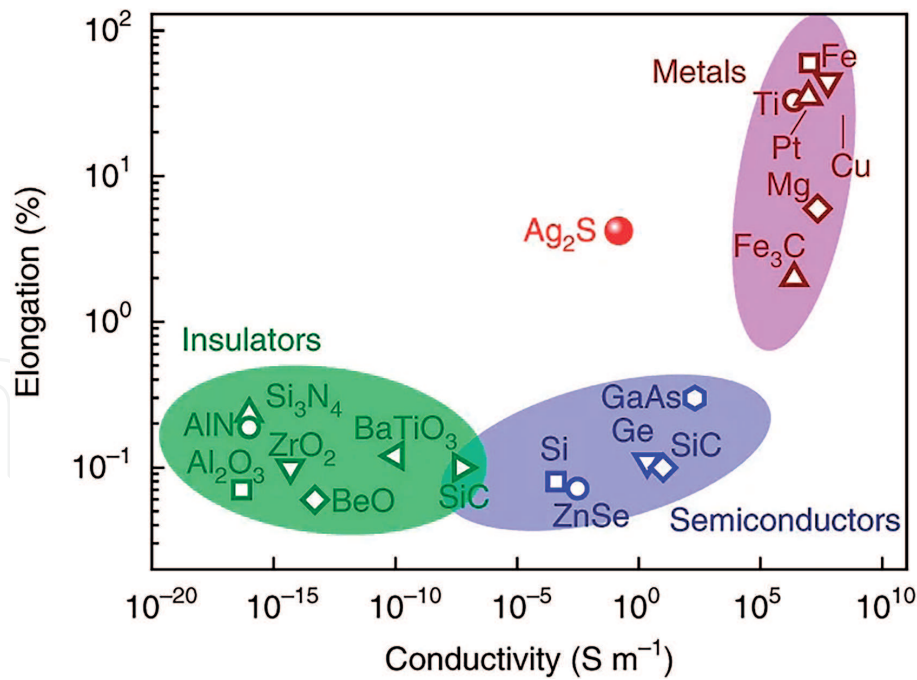


**Figure 5.** Elongation versus electrical conductivity for  $\alpha$ - $\text{Ag}_2\text{S}$  and various materials. Adapted from Ref. [21] with permissions from Springer Nature, Copyright 2018.

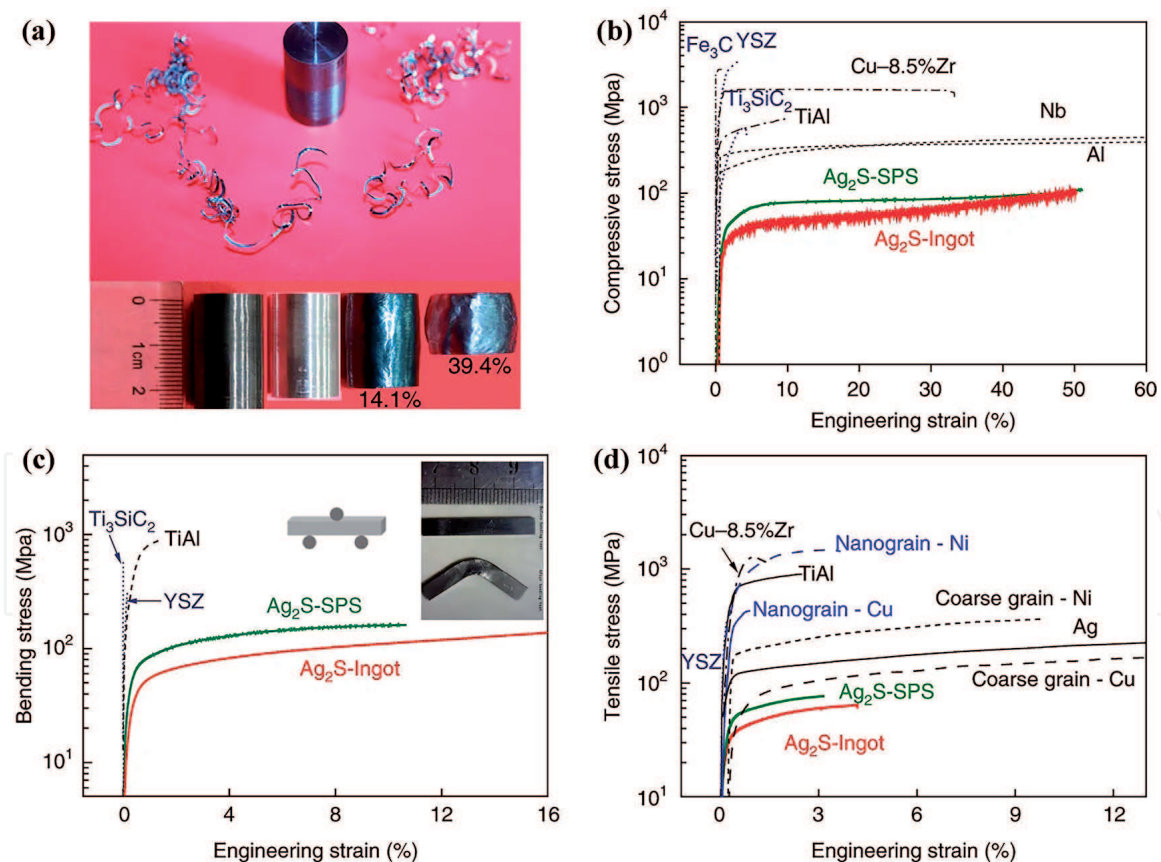


**Figure 6.** Room-temperature mechanical properties of the semiconductor  $\alpha$ - $\text{Ag}_2\text{S}$ . (a) A machined cylinder for the compression test (top) and its deformations under hammering (bottom). (b–d) Strain-stress curves for compression (b), bending, (c) and tension (d) tests at room temperature. Typical materials such as the ceramics yttria-stabilized zirconia (YSZ) and Ti, SiC; the metals Al, Nb, Ni, Cu, Ag, Cu–8.5%Zr alloy, and  $\text{Fe}_3\text{C}$ ; and the intermetallic compound TiAl are shown for comparison. The inset in c shows the as-cast ingot samples before and after the bending test. Adapted from Ref. [21] with permissions from Springer Nature, Copyright 2018.

tetramolecular units. Four S and four Ag atoms constitute eight-atomic ring fragments interlinked by the sulfur atoms. Precisely among (100) plane, a wrinkled structure formed by two S and six Ag atoms stacking along [100] direction, and this structure provides channels for slipping. In addition, it was found that Ag sites were occupied only for 70%, while S sites occupied completely. These unfixed Ag atoms may induce additional Ag-S and Ag-Ag bonds.

The multicentered, diffuse, and relatively weak bonding gives rise to the small slipping energy and large cleavage energy, i.e., plastic material can slip easily without cleavage as shown in **Figure 7**. As for  $\alpha$ -Ag<sub>2</sub>S, it is assumed that slip plane is (100) and slip direction [001]. According to the calculation, the slipping energy ( $E_B$ ) is 150 meV per atom for Ag<sub>2</sub>S, which is comparably small with conventionally ductile metals (Ti, Mg); also, the cleavage energy is relatively large for Ag<sub>2</sub>S, which is 148 meV per atom, indicating certain relatively strong forces interlinking those slip planes instead of cleaving. In comparison, the values are, respectively, less than 60 meV for NaCl, graphite, and diamond; 570 meV for Mg; and 2150 meV per atom for Ti.

The distribution of the electron localizability indicator (ELI-D) shows a local maximum on the outer side of each S atom, and the basin of this maximum is caused by the formation of a lone pair or a strong Ag-S interaction shown in quantum theory of atoms in molecules (QTAIM). Besides, these lone pairs form double layers in the (100) plane. Thus, the  $E_B$  is supposed to be small due to a relative weak interaction between the lone pairs. The COHP calculations reveal chemical bonds changing during the glide. During the slipping process, some bonds vanish, while new bonds form continuously during the whole process, and these new bonds are comparable with the Ag-S bonds between layers in strength. Therefore, S atoms are always bonded with Ag atoms, resulting in a large  $\Delta E_C$  to prevent materials from cleaving. In short, S atoms move along Ag-formed tracks easily due to small energy difference in steps, while these are difficult to cleavage for tight bonding with surrounded Ag atoms.

Li et al. [37] applied *ab initio*-based DFT to investigate the structural response of Ag<sub>2</sub>S under pure shear, uniaxial tension, and biaxial shear deformations. To simulate quasi-static mechanical loading process, they imposed shear or tensile strain on a particular system gradually. It is found that Ag<sub>2</sub>S has a theoretical shear strength of 1.02 GPa in the (001) [010] and (100) [010] slip systems (**Figure 8(a)**) lower than that of common metal and ceramics. The ideal tensile strength along [100] direction is 2.2 GPa, significantly higher than its shear strength (**Figure 8(b)**). The very low shear strength under these slip systems is expected to create pathways for easy slip.

The Ag-S octagon structure would be highly distorted under shear deformation. However, the Ag-S bond lengths change only slightly during shearing. Only when the strain is larger than ~110%, bond breakage would happen. This feature implies that Ag<sub>2</sub>S would retain its structural integrity even under very large shear deformation. Under (100) [010] shear load, Ag-Ag metallic bonds would form at 0.671 strain. These newly formed bonds strengthen the Ag-S frameworks and contribute to its structural integrity. Under [100] tensile load, the processes of breakage and the formation of Ag-S bond happen at the same time. The structural integrity could thus be preserved to a large strain. Based on these discoveries, they proposed that the easy slip pathways with good structural integrity under shear load are the origin of ductility in Ag<sub>2</sub>S.

Recent research also found that the single-layer Ag<sub>2</sub>S is a kind of auxetic materials with unusual negative Poisson's ratio [38]. According to their calculations, single-layer Ag<sub>2</sub>S has relatively low Young's modulus with 61.61 N·m<sup>-1</sup> along [010] direction and 2.78 N·m<sup>-1</sup> along [100] direction. This is the lowest value found in various 2D materials such as graphite and MoS<sub>2</sub>. This means that along [100] direction, single-layer Ag<sub>2</sub>S will show extraordinary flexibility. Moreover, single-layer Ag<sub>2</sub>S shows negative Poisson's ratio in both in-plane and out-of-plane directions, which is unique among quasi-2D materials.

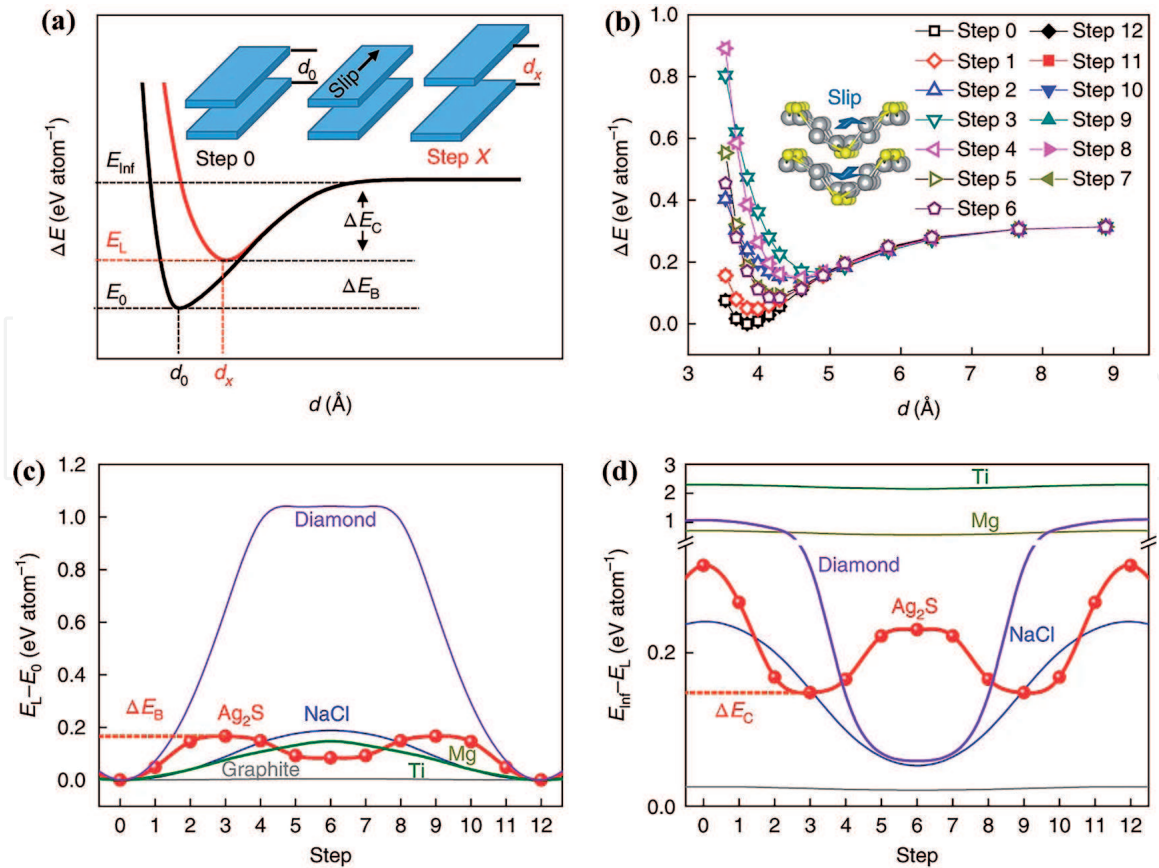


**Figure 7.** (a) Crystal structure of  $\alpha$ -Ag<sub>2</sub>S along [001] direction. (b) Schematic map for energy variation as a function of interlayer distance  $d$  during slipping. (c) ( $E_L - E_0$ ) and (d) ( $E_{inf} - E_L$ ) behavior during slipping. Adapted from Ref. [21] with permissions from Springer Nature, Copyright 2018.

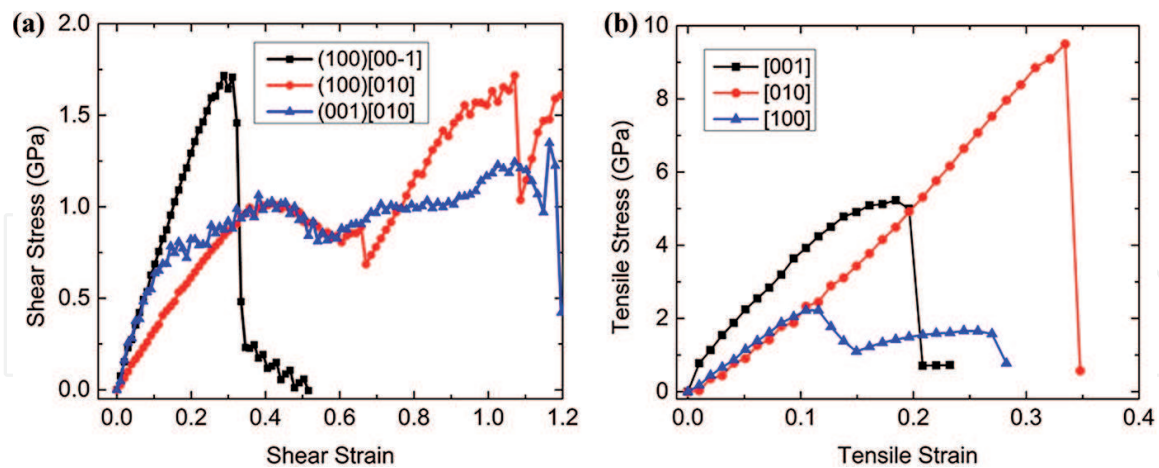


**Figure 8.** Stress response of  $\alpha$ -Ag<sub>2</sub>S against pure shear strain and biaxial tensile strain, respectively. (a) Shear-stress-shear-strain relations along various slip systems. (b) Tensile-stress-tensile-strain relations along various tensile systems. Adapted from Ref. [37] under the Creative Commons CC BY license.

## 7. Full inorganic flexible thermoelectric materials

The discovery of plastic Ag<sub>2</sub>S makes it possible to fabricate full-inorganic flexible devices. Pristine Ag<sub>2</sub>S exhibits a medium band gap ( $\sim 1.0$  eV), high mobility ( $\sim 100$  cm<sup>2</sup>/Vs), and extremely low lattice thermal conductivity ( $\sim 0.5$  Wm<sup>-1</sup>K<sup>-1</sup> near room temperature) [21], which makes it a potential candidate

for thermoelectric application. However, the extremely low carrier concentration (about  $1.6 \times 10^{14} \text{ cm}^{-3}$  at room temperature) leads to its poor electrical conductivity. Therefore, the thermoelectric performance of  $\text{Ag}_2\text{S}$  should be further optimized, and its plasticity should be maintained at the same time.

By alloying with Se/Te, Liang et al. successfully tuned the carrier concentration of  $\text{Ag}_2\text{S}$  by virtue of the lowered defect formation energy of Ag interstitial atoms. Consequently, the electrical conductivity and power factor were largely optimized: the electrical conductivities of  $\text{Ag}_2\text{S}_{0.5}\text{Se}_{0.5}$ ,  $\text{Ag}_2\text{S}_{0.8}\text{Te}_{0.2}$ , and  $\text{Ag}_2\text{S}_{0.5}\text{Se}_{0.45}\text{Te}_{0.05}$  reach around  $10^4 \text{ S m}^{-1}$  at room temperature, which are comparable to state-of-the-art brittle inorganic TE materials. The power factors of  $\text{Ag}_2\text{S}$ -based materials can reach  $5 \mu\text{W}\cdot\text{cm}^{-1}\cdot\text{K}^{-2}$  at room temperature. Meanwhile,  $\text{Ag}_2(\text{S}, \text{Se})$ ,  $\text{Ag}_2(\text{S}, \text{Te})$ , and  $\text{Ag}_2(\text{S}, \text{Se}, \text{Te})$  have record low thermal conductivities of  $0.3\sim 0.6 \text{ Wm}^{-1} \text{ K}^{-1}$  at  $300\sim 450 \text{ K}$ , among the lowest values observed in fully densified inorganic solids. The band gap of Se or Te alloyed  $\text{Ag}_2\text{S}$ -based materials is also reduced, shifting the peak value of  $zT$  toward a lower temperature. Thus, a highest  $zT$  value about 0.44 could be realized for  $\text{Ag}_2\text{S}_{0.5}\text{Se}_{0.45}\text{Te}_{0.05}$  at room temperature.

More interestingly, alloying does not severely impair the plasticity. According to the mechanical property test, the ductility and flexibility of  $\text{Ag}_2\text{S}$ -based materials would be maintained if the Se content is less than 60% or the Te content is less than 70%. Hence, the materials would possess both good ductility and TE performance when the Se/Te content is in the range of  $20\sim 60\%$ , as shown in **Figure 9(c)**. To further verify the robustness of  $\text{Ag}_2\text{S}$ -based materials under different usage scenarios, bending cycle test was conducted on  $\text{Ag}_2\text{S}_{0.5}\text{Se}_{0.5}$  strip with a thickness of about  $10 \mu\text{m}$ . As shown in **Figure 9(f)**, the variation in Seebeck coefficient and electrical conductivity is less than 10% after 1000 bending cycles with a bending radius less than  $3 \text{ mm}$ . In addition, the relative resistance variation in the strip under different bending radius is also estimated.

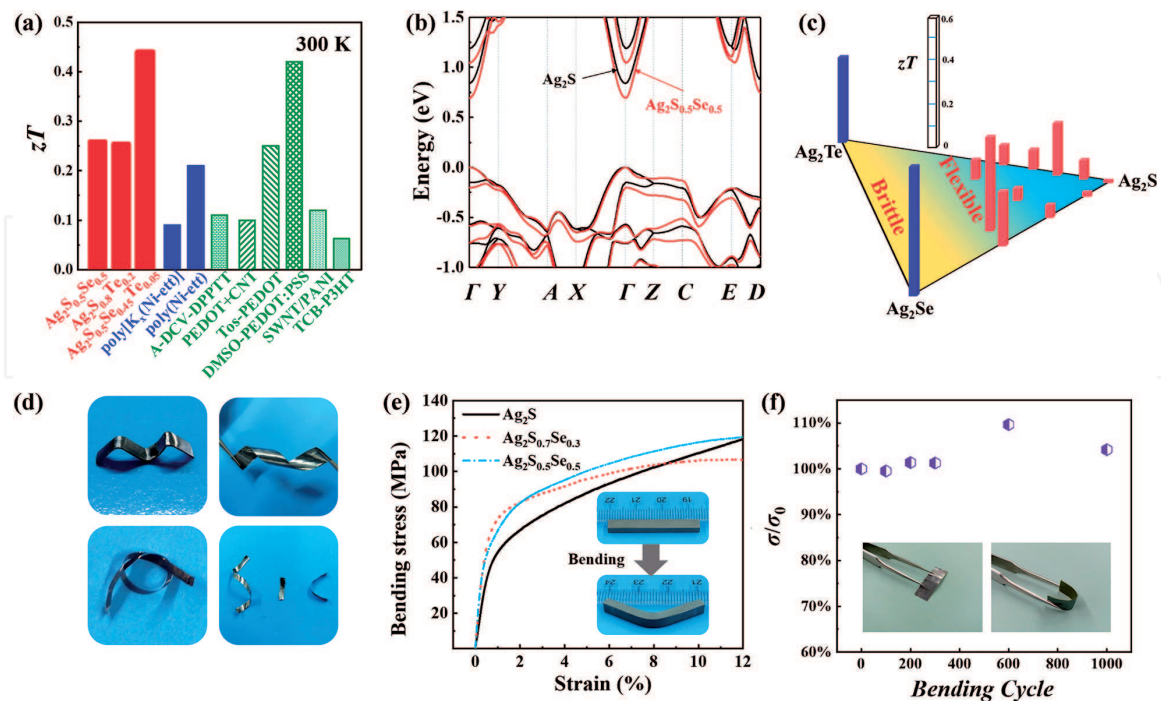


**Figure 9.**

(a) TE figure of merit  $zT$  for  $\text{Ag}_2(\text{S}, \text{Se})$ ,  $\text{Ag}_2(\text{S}, \text{Te})$ , and  $\text{Ag}_2(\text{S}, \text{Se}, \text{Te})$  at 300 K. Several representative organic TE materials are included for comparison. (b) Calculated band structure for  $\text{Ag}_2\text{S}$  and  $\text{Ag}_2\text{S}_{0.5}\text{Se}_{0.5}$ . (c) Flexibility- $zT$  phase diagram of  $\text{Ag}_2\text{S}$ - $\text{Ag}_2\text{Se}$ - $\text{Ag}_2\text{Te}$  system. (d) The  $\text{Ag}_2\text{S}_{0.5}\text{Se}_{0.5}$  and  $\text{Ag}_2\text{S}_{0.8}\text{Te}_{0.2}$  samples twisted to various shapes. (e) Bending tests of  $\text{Ag}_2\text{S}_{1-x}\text{Sex}$  ( $x = 0, 0.1, 0.3, 0.5$ ). (f) Relative electrical conductivity variation  $\sigma/\sigma_0$  of the  $\text{Ag}_2\text{S}_{0.5}\text{Se}_{0.5}$  foil after various number of times of bending cycles. Reproduced from Ref. [22] with permissions from The Royal Society of Chemistry. Copyright 2019.

Using  $\text{Ag}_2\text{S}_{0.5}\text{Se}_{0.5}$  strips as  $n$ -type legs and Pt-Rh wires as  $p$ -type legs, full-inorganic thermoelectric devices were fabricated as shown in **Figure 10** [22]. Under temperature difference 20 K, the maximum power of the device is 10  $\mu\text{W}$ , and the normalized maximum power density  $P_{\text{max}}L/A$  reaches  $0.08 \text{ W}\cdot\text{m}^{-1}$ , which is much higher than those for current organic TE devices. This research has solved the most fundamental and challenging problems for the fabrication of full-inorganic and high-performance flexible thermoelectrics, opening a new direction for inorganic flexible thermoelectrics.

The conventional strategy toward flexible TE devices is mounting TE thin-film materials onto the intrinsically flexible substrates. Ding et al. [39] fabricated flexible TE devices based on  $\text{Ag}_2\text{Se}$  nanowires and plastic nylon substrate. The hybrid film was hot pressed at  $200^\circ\text{C}$  and 1 MPa for 30 min, which endows the film high TE performance and excellent flexibility at the same time. The highest power factor value of as-prepared  $\text{Ag}_2\text{Se}/\text{nylon}$  film reaches  $9.87 \mu\text{Wm}^{-1} \text{K}^{-2}$  at 300 K, almost the highest value among reported  $n$ -type flexible TE materials. Although the internal resistance of the four legs of  $\text{Ag}_2\text{Se}/\text{nylon}$  devices is up to  $250 \Omega$ , the in-plane TE device exhibits a high-power density of  $2.3 \text{ W m}^{-2}$  under a temperature difference of 30 K.

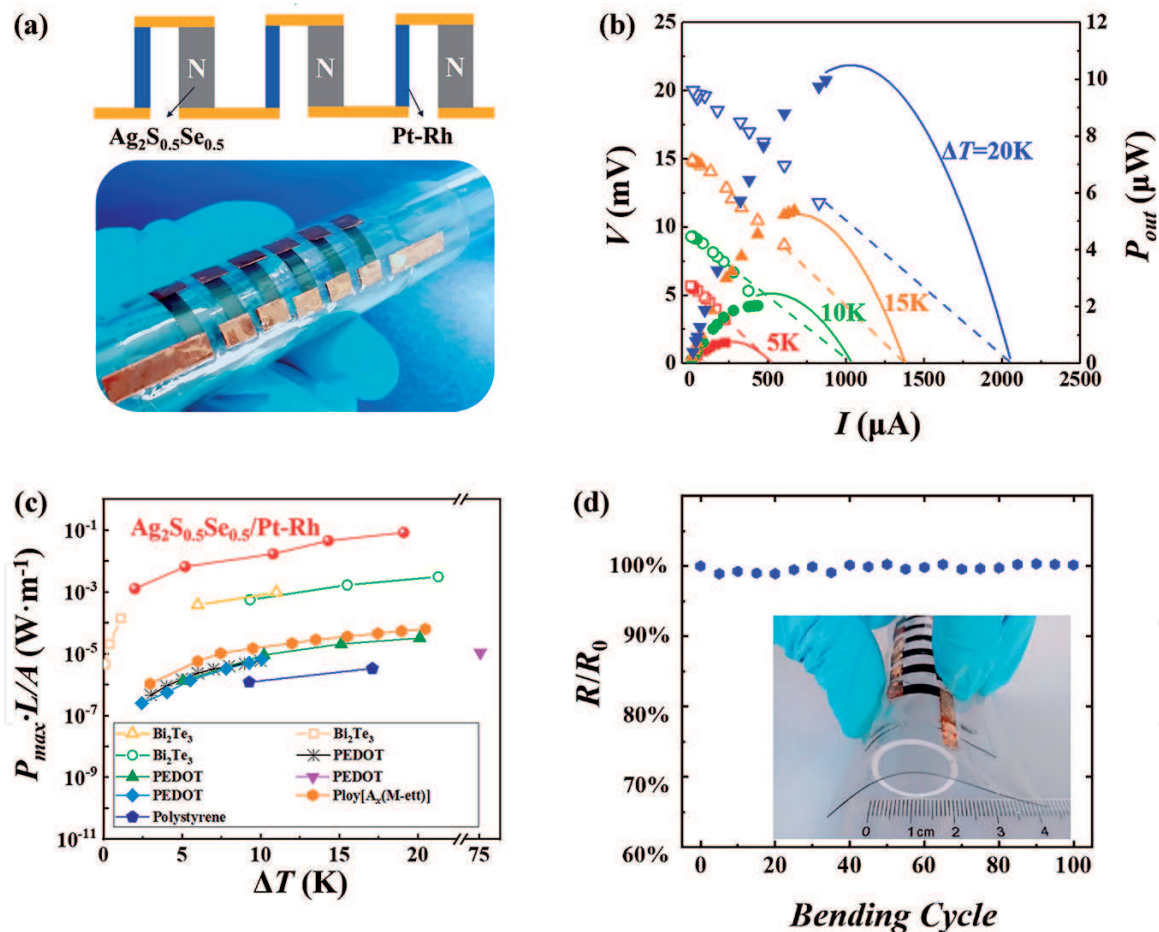


**Figure 10.** (a) Upper panel: A schematic of the  $\text{Ag}_2\text{S}_{0.5}\text{Se}_{0.5}/\text{Pt-Rh}$  in-plane device with  $\text{Ag}_2\text{S}_{0.5}\text{Se}_{0.5}$  as  $n$ -type legs and Pt-Ru wire as  $p$ -type legs. Bottom panel: Optical image of a six-couple flexible  $\text{Ag}_2\text{S}_{0.5}\text{Se}_{0.5}/\text{Pt-Rh}$  TE device. The as-shown in-plane device is merely for the purpose of demonstration. (b) Output voltage  $V$  and power output  $P_{\text{out}}$  as a function of current ( $I$ ) for a six-couple  $\text{Ag}_2\text{S}_{0.5}\text{Se}_{0.5}/\text{Pt-Rh}$  device under different operating temperature differences. The cold side temperature is fixed at 293 K. (c) Comparison of normalized maximum power density ( $P_{\text{max}}L/A$ ) among the  $\text{Ag}_2(\text{S}, \text{Se})$ -based inorganic TE device, inorganic-organic hybrid flexible TE devices, and organic flexible TE devices. (d) Relative electrical resistance variation  $R/R_0$  of the  $\text{Ag}_2\text{S}_{0.5}\text{Se}_{0.5}/\text{Pt-Rh}$  TE device after bending various number of times. The inset shows the optical image for the bended device. The bending radius is 10 mm. Reproduced from Ref. [22] with permissions from The Royal Society of Chemistry. Copyright 2019.

## 8. Summaries and outlook

This chapter reviews the newly emerging plastic inorganic semiconductors (e.g.,  $\text{Ag}_2\text{S}$ ) for next-generation flexible electronics. The term “flexibility” is clarified at the very beginning. It should be recognized that plasticity is important for flexible electronics due to the availability of feasible processing and deformability free of size restricts. The intrinsic brittleness for inorganic semiconductors and ceramics is explained from unidirectional and saturated characteristics of covalent bonds. Historically, ionic crystals like  $\text{AgCl}$  have been found to exhibit certain plasticity but lack decent electrical conductivity. Groundbreakingly,  $\text{Ag}_2\text{S}$  was discovered as the room-temperature ductile semiconductor. From the chemical bonding perspective, the multicentered, diffuse, weak interactions induce easy slipping while maintaining the integrity, which holds well not only for  $\text{Ag}_2\text{S}$  but also for other plastic materials. The generalized bonding features are useful guidance for developing new flexible/plastic semiconductors. The electrical properties and thermoelectric performance of  $\text{Ag}_2\text{S}$  are readily optimized upon Se/Te alloying while maintaining the plasticity and flexibility. Successively, full-inorganic thermoelectric devices are fabricated based on plastic and flexible  $\text{Ag}_2\text{S}$ -based semiconductors, yielding much higher output power density than organic counterparts.

The discovery and application demonstration of plastic  $\text{Ag}_2\text{S}$  inorganic semiconductor pave a new way toward next-generation flexible electronics. Facing large-scale applications in electronics and energy conversions, several key challenges lie ahead. First and basically, the mechanisms for plastic deformation in  $\text{Ag}_2\text{S}$  needs further investigation, especially on the individual and synergetic effects of both chemical bonding and dislocations, which calls for tremendous efforts of both experimentalists and theorists from a variety of disciplines. Second, practical criteria are required to rapidly screen potentially new, plastic/flexible semiconductors. These performance indicators should be easily available yet insightful, and it is better that they can be implemented into the high-throughput calculations. Third, all the techniques are to be renewed including material processing, electrode/substrate selection, device fabrication, and circuit integration.

Facing all these exciting challenges and fascinating opportunities, there is no doubt that the flexible/plastic inorganic semiconductors will bring a revolution to academic communities, electronic/energy industries, and worldwide market. The next-generation flexible electronics is meant to deeply change our life and reshape the world. The future has come.

IntechOpen

### Author details

Tian-Ran Wei<sup>1,2</sup>, Heyang Chen<sup>2</sup>, Xun Shi<sup>1,2</sup> and Lidong Chen<sup>1\*</sup>

1 State Key Laboratory of High Performance Ceramics and Superfine Microstructure, Shanghai Institute of Ceramics, Chinese Academy of Sciences, Shanghai, China

2 State Key Laboratory of Metal Matrix Composites, School of Materials Science and Engineering, Shanghai Jiao Tong University, Shanghai, China

\*Address all correspondence to: [cld@mail.sic.ac.cn](mailto:cld@mail.sic.ac.cn)

### IntechOpen

© 2020 The Author(s). Licensee IntechOpen. This chapter is distributed under the terms of the Creative Commons Attribution License (<http://creativecommons.org/licenses/by/3.0>), which permits unrestricted use, distribution, and reproduction in any medium, provided the original work is properly cited. 

## References

- [1] Wong WS, Salleo A. Flexible Electronics: Materials and Applications. Vol. 11. New York: Springer Science & Business Media; 2009
- [2] Kim D-H, Lu N, Ma R, Kim Y-S, Kim R-H, Wang S, et al. Epidermal electronics. *Science*. 2011;**333**(6044): 838-843
- [3] Gates BD. Flexible electronics. *Science*. 2009;**323**(5921):1566-1567
- [4] Sun Y, Rogers JA. Inorganic semiconductors for flexible electronics. *Advanced Materials*. 2007;**19**(15):1897-1916
- [5] Cavallo F, Lagally MG. Semiconductors turn soft: Inorganic nanomembranes. *Soft Matter*. 2010;**6**(3):439-455
- [6] Rogers JA, Lagally MG, Nuzzo RG. Synthesis, assembly and applications of semiconductor nanomembranes. *Nature*. 2011;**477**(7362):45-53
- [7] Kaltenbrunner M, Sekitani T, Reeder J, Yokota T, Kuribara K, Tokuhara T, et al. An ultra-lightweight design for imperceptible plastic electronics. *Nature*. 2013;**499**(7459): 458-463
- [8] Zhang S, Xu X, Lin T, He P. Recent advances in nano-materials for packaging of electronic devices. *Journal of Materials Science: Materials in Electronics*. 2019;**30**:13855-13868
- [9] Yang M, Kim SW, Zhang S, Park DY, Lee C-W, Ko Y-H, et al. Facile and highly efficient fabrication of robust Ag nanowire-elastomer composite electrodes with tailored electrical properties. *Journal of Materials Chemistry C*. 2018;**6**(27):7207-7218
- [10] Xu J, Wang S, Wang G-JN, Zhu C, Luo S, Jin L, et al. Highly stretchable polymer semiconductor films through the nanoconfinement effect. *Science*. 2017;**355**(6320):59-64
- [11] Sekitani T, Yokota T, Zschieschang U, Klauk H, Bauer S, Takeuchi K, et al. Organic nonvolatile memory transistors for flexible sensor arrays. *Science*. 2009;**326**(5959):1516-1519
- [12] Oh JY, Rondeau-Gagne S, Chiu YC, Chortos A, Lissel F, Wang GN, et al. Intrinsically stretchable and healable semiconducting polymer for organic transistors. *Nature*. 2016;**539**(7629):411-415
- [13] Jin ML, Park S, Kim JS, Kwon SH, Zhang S, Yoo MS, et al. An ultrastable ionic chemiresistor skin with an intrinsically stretchable polymer electrolyte. *Advanced Materials*. 2018;**30**(20):1706851
- [14] Timoshenko SP, Woinowsky-Krieger S. *Theory of Plates and Shells*. Auckland: McGraw-hill; 1959
- [15] Bhimanapati GR, Lin Z, Meunier V, Jung Y, Cha J, Das S, et al. Recent advances in two-dimensional materials beyond graphene. *ACS Nano*. 2015;**9**(12):11509-11539
- [16] Fiori G, Bonaccorso F, Iannaccone G, Palacios T, Neumaier D, Seabaugh A, et al. Electronics based on two-dimensional materials. *Nature Nanotechnology*. 2014;**9**:768-779
- [17] Lee C, Wei X, Kysar JW, Hone J. Measurement of the elastic properties and intrinsic strength of monolayer graphene. *Science*. 2008;**321**(5887):385-388
- [18] Kim J, Kim J, Song S, Zhang S, Cha J, Kim K, et al. Strength dependence of epoxy composites on the average filler size of non-oxidized graphene flake. *Carbon*. 2017;**113**:379-386

- [19] Faber KT, Malloy KJ. *The Mechanical Properties of Semiconductors*. San Diego: Academic Press; 1992
- [20] Green DJ. *An Introduction to the Mechanical Properties of Ceramics*. Cambridge: Cambridge University Press; 1998
- [21] Shi X, Chen H, Hao F, Liu R, Wang T, Qiu P, et al. Room-temperature ductile inorganic semiconductor. *Nature Materials*. 2018;**17**:421-426
- [22] Liang J, Wang T, Qiu P, Yang S, Ming C, Chen H, et al. Flexible thermoelectrics: From silver chalcogenides to full-inorganic devices. *Energy & Environmental Science*. 2019;**12**(10):2983-2990
- [23] Peng J, Snyder GJ. A figure of merit for flexibility. *Science*. 2019;**366**(6466):690-691
- [24] Lu Q, Arroyo M, Huang R. Elastic bending modulus of monolayer graphene. *Journal of Physics D: Applied Physics*. 2009;**42**(10):102002
- [25] Yu PY, Cardona M. *Fundamentals of Semiconductors*. Berlin: Springer; 2010
- [26] Zeier WG, Zevalkink A, Gibbs ZM, Hautier G, Kanatzidis MG, Snyder GJ. Thinking like a chemist: Intuition in thermoelectric materials. *Angewandte Chemie, International Edition*. 2016;**55**(24):2-18
- [27] Nye JF. Plastic deformation of silver chloride I. internal stresses and the glide mechanism. *Proceedings of the Royal Society of London, Series A: Mathematical, Physical and Engineering Sciences*. 1949;**198**(1053):190-204
- [28] Nye JF. Plastic deformation of silver chloride. II. Photoelastic study of the internal stresses in glide packets. *Proceedings of the Royal Society of London. Series A: Mathematical and Physical Sciences*. 1949;**200**(1060):47-66
- [29] Stoloff N, Lezius D, Johnston T. Effect of temperature on the deformation of KCl-KBr alloys. *Journal of Applied Physics*. 1963;**34**(11):3315-3322
- [30] Taylor A, Albers H, Pohl R. Effect of plastic deformation on the thermal conductivity of various ionic crystals. *Journal of Applied Physics*. 1965;**36**(7):2270-2278
- [31] Skrotzki W, Frommeyer O, Haasen P. Plasticity of polycrystalline ionic solids. *Physica Status Solidi*. 1981;**66**(1):219-228
- [32] Vávra F, Ševčík Z. Formation of wavy slip bands in AgCl crystals at low temperatures. *Czechoslovak Journal of Physics B*. 1986;**36**(4):509-513
- [33] Stokes R, Li C. Dislocations and the strength of polycrystalline ceramics. In: Stadelmaier HH, Austin WW, editors. *Materials Science Research*. Boston: Springer; 1963. pp. 133-157
- [34] Nakamura A, Ukita M, Shimoda N, Furushima Y, Toyoura K, Matsunaga K. First-principles calculations on slip system activation in the rock salt structure: Electronic origin of ductility in silver chloride. *Philosophical Magazine*. 2017;**97**(16):1281-1310
- [35] Ukita M, Nakamura A, Yokoi T, Matsunaga K. Electronic and atomic structures of edge and screw dislocations in rock salt structured ionic crystals. *Philosophical Magazine*. 2018;**98**(24):2189-2204
- [36] Oshima Y, Nakamura A, Matsunaga K. Extraordinary plasticity of an inorganic semiconductor in darkness. *Science*. 2018;**360**(6390):772-774
- [37] Li G, An Q, Morozov SI, Duan B, Goddard WA, Zhang Q, et al.

Ductile deformation mechanism  
in semiconductor  $\alpha$ -Ag<sub>2</sub>S. npj  
Computational Materials. 2018;**4**(1):44

[38] Peng R, Ma Y, He Z, Huang B,  
Kou L, Dai Y. Single-layer Ag<sub>2</sub>S: A  
two-dimensional bidirectional Auxetic  
semiconductor. Nano Letters.  
2019;**19**(2):1227-1233

[39] Ding Y, Qiu Y, Cai K, Yao Q,  
Chen S, Chen L, et al. High performance  
n-type Ag<sub>2</sub>Se film on nylon membrane  
for flexible thermoelectric power  
generator. Nature Communications.  
2019;**10**(1):841

IntechOpen